CARDBOARD PANELS REINFORCED WITH BRAIDED UNIDIRECTIONAL GLASS RODS FOR VEHICLE CRASH IMPACT ATTENUATION

Gabriel Fortin[1], Yuri Imai[1] and Hiroyuki Hamada[2]

[1] The Department of Advanced-Fibro Science, Kyoto Institute of Technology, Matsugasaki, Sakyo-ku, Kyoto, 606-8585, Japan

[2] The Future-Applied Conventional Technology Centre, Kyoto Institute of Technology, Matsugasaki, Sakyo-ku, Kyoto, 606-8585, Japan

Keywords: Crashworthiness, Braiding, Cardboard, Glass fiber rods, Progressive crushing

ABSTRACT

In this study, cardboard panels are reinforced with unidirectional glass fiber rods covered with a braided glass fiber sleeve for use as a vehicle crash impact attenuation structure. The goal is to create a structural panel to be incorporated in a rally car roll cage for side impact protection. There is growing interest in implementing cardboard materials in structural panels due to its vast availability, low density, low cost, and use of recycled paper. The crushing properties of braided unidirectional glass rods have been previously studied extensively. Braided rods show excellent crushing characteristics in the form of progressive crushing where the load remains relatively constant throughout crushing. The rods consist of unidirectional glass fibers in the axial direction covered by a layer of braided glass fibers. The axial fiber bundles are covered with the braided glass fiber bundles using an industrial tubular braiding machine. The braided preform is then impregnated in resin under vacuum conditions, and then hung inside an oven throughout curing. Rods with a diameter of 3.4 mm and a height of 11 mm are manufactured in this study. The crash panels involve arranging the rods vertically through the thickness of a cardboard panel, with the axis of the rods spanning through the entire thickness of the cardboard and aligned parallel to the crushing load direction. Variations in the number of rods are studied. The crushing properties are investigated, and the effects of the cardboard on the failure mechanisms of the rods are analyzed.

1 INTRODUCTION

Approximately 60 million cars are produced in the world every year [1], and the transportation sector accounts for approximately 27 percent of all global greenhouse gas emissions [2]. In addition, a recent study in the United States has shown that the annual deaths caused by road pollution alone now exceeds that caused by traffic accidents [3]. In 2015, there was an estimated 38,300 traffic accident deaths in the United States [4]. Evidently, one of the major challenges that we face is to make the automobiles of the future both safer and more environmentally-friendly. Designing automotive structures that are both light and strong is critical for reducing fuel consumption and the associated CO_2 emissions as well as ensuring safety and effective crashworthiness. Crashworthiness and impact energy management of automotive structures is a key topic related to automobile safety. As part of a project for manufacturing lightweight crash attenuation panels for side impact protection of a professional rally car, a thin structure based on corrugated cardboard panels and braided unidirectional glass fiber rods is being developed and tested.

The energy absorption properties of composite tubes and rods have previously been studied by Hamada et al. [5, 6], and Hull [7]. They have found that when designed properly, composite tubes possess superior crushing characteristics to metals. Compression of metal tubes generally leads to a phenomenon known as progressive folding, as illustrated in fig. 1 [7] where the load oscillates about a constant mean value as the metal edges of the tube fold over. The typical load-displacement curve involves a load that is rapidly increasing to a maximum value, followed by a drop to the mean load

value where progressive folding occurs. Progressive folding takes place until the metal tube is completely compressed, after which the load increases during material compaction. It is because of progressive folding that metal tubular structures are quite stable in compression and possess good crushing characteristics.

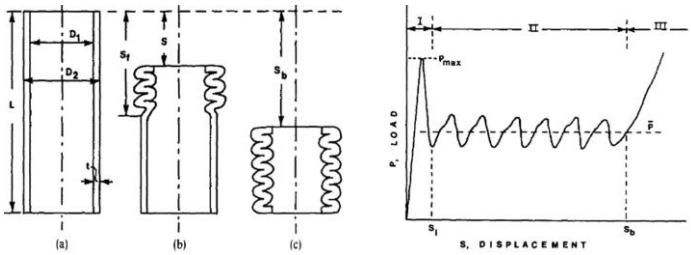

Figure 1: Schematic representation of progressive folding (left), and typical load-displacement curve for progressive folding (right): i, fold initiation; ii, progressive folding; iii, compaction. [7]

Hamada et al. [5-6] and Hull [7] have shown that when designed properly, composite tubes also exhibit a stable crushing phenomenon known as progressive crushing, not to be confused with progressive folding in metals. During progressive crushing of composites, tubes that are designed with a trigger at one end such as a chamfer angle will exhibit progressive crushing behavior. Progressive crushing of a composite tube is illustrated in fig. 2. During crushing of the chamfer, the load increases to a maximum value, and then drops to a constant mean load where progressive crushing takes place. Progressive crushing occurs until the material in the tube is fully compressed. Instead of folding that is typical in metals, composite tubes exhibit fiber splaying outwards from the chamfer end. The outward splaying of fibers is a clear sign that an optimal amount of energy is being absorbed during compression. In compression, it is common to express a specific energy absorption value, presented in eq. (1) as:

$$E_s = \frac{\overline{P}}{A\rho} \tag{1}$$

Where E_s is the specific energy absorption, $\overline{P}$ is the mean load during progressive crushing, A is the cross-sectional area of the structure, and ρ is the density of the structure. E_s is typically expressed in kJ/kg. Hamada et al. [6] have shown that the specific energy of composite tubes made from strong reinforcing fibers and a tough matrix such as carbon/PEEK have far superior specific energy absorption to metals. They have reported E_s values of 225 kJ/kg for carbon fiber/PEEK, 82.1 kJ/kg for carbon fiber/epoxy, 53.7 kJ/kg for glass fiber/epoxy, and 33.7 and 66.9 kJ/kg for steel and aluminum, respectively.

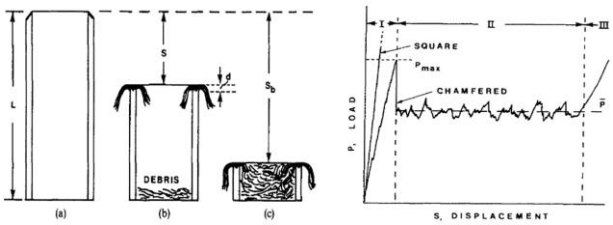

Figure 2: Schematic representation of progressive crushing (left), and typical load-displacement curve of a tube with chamfered end undergoing progressive crushing (right): i, formation of crush zone; ii, progressive crushing, compaction of debris. [7]

Hamada et al. [6] have also shown very similar behavior in composite rods that are approximately 12 mm in diameter, specifically in braided glass fiber composite rods consisting of axial fibers at the core covered by braided fibers. Braided fabrics are a type of textile preform that consist of continuous fiber bundles, ensuring that all fibers can sustain loads resulting in superior mechanical properties. The

continuous fiber architecture of braided structures also makes them very suitable for pre-forming complex three-dimensional shapes that cannot be produced otherwise [6].

They have found that the rods perform well in compression and exhibit progressive crushing. They have studied the effect of the braiding angle, number of fiber bundles, and the effect of the ratio of hoop fibers to axial fibers on the specific energy absorption. Hull [7] has suggested that cracks that develop within the axial fibers are prevented by the hoop fibers that apply a radial compressive stress. The combination of axial and hoop fibers therefore results in excellent crushing characteristics. The ratio of virtual hoop fibers to axial fibers in a braided rod can be calculated from eq. (2):

$$\frac{H_f}{A_f} = \frac{N_b sin(\alpha)}{N_a + N_b cos(\alpha)} \tag{2}$$

Where H_f is the number of virtual hoop fibers, A_f is the number of virtual axial fibers, N_b is the total number of braiding fibers, N_a is the total number of axial fibers, and α is the braiding angle. By changing the parameters in eq. (2), the H_f/A_f ratio can be varied. Hamada et al. [6] have studied the relationship between the H_f/A_f ratio and the specific energy absorption for braided glass fiber rods, and found that there is an optimal value in the range of H_f/A_f = 0.12 to 0.13 (resulting in an energy absorption value of approximately 70 kJ/kg). The rods showed progressive crushing behavior in the form of fiber splaying.

Yasuda et al. [8] also performed compression tests on 12 mm-diameter braided glass fiber composite rods, and studied the effects of the number of braiding layers surrounding the axial core, and the effect of a taper angle. He showed an increase in the mean load of the samples with increasing number of braided layers. In addition, rods with a taper angle performed much better than rods with no taper angle. The taper angle in a composite rod acts the same way as a chamfer in a composite tube. The taper involves grinding one end of the rod at a specified angle to a fine tip.

This paper focuses on the crushing behaviour of small braided glass fiber rods that are inserted inside a corrugated cardboard panel. The first portion of this work involved manufacturing the rods from a braided and axial glass fiber preform using a tubular braiding machine. The fiber preform was subsequently impregnated with epoxy resin and cured to its final shape. Then, the rods were inserted into the cardboard panels, at specific locations. The crushing properties of cardboard panels with 0, 1, and 4 rods were studied. The progressive crushing behavior of the panels are evaluated from the compression load-displacement curves, and the failure of the rods within the cardboard is examined visually and by optical microscopy.

2 EXPERIMENTAL METHODS

2.1 Material Specifications

A corrugated cardboard sample and its dimensions that was used for compression testing in this study is included in fig. 3-A. The cardboard samples consisted of 2 layers, with dimensions of 60 mm × 60 mm × 12 mm. All samples were cut to size using a high-speed cutter.

An example of a manufactured braided unidirectional glass rod is presented in fig. 3-B. The rods are approximately 3.4 mm in diameter, 11.1 mm in length, and include a 45° taper angle. All rods were made with the same taper angle in this study. The core of the rod consists of unidirectional glass fibers (16 axial fiber bundles) covered by braided glass fibers (8 axial fiber bundles). The fibers for the axial and braiding portions of the rod (type RS 57QM-521, tex = 575 g/1000 m) have been provided by Nitto Boseki Co., Ltd. The braiding angle is 45°.

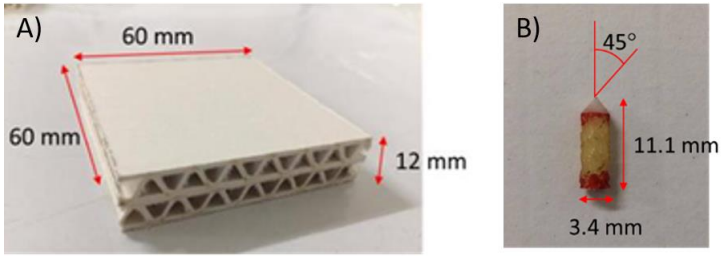

Figure 3: A) Corrugated cardboard sample and dimensions (for thru-thickness compression testing); B) Manufactured braided unidirectional glass rod for reinforcing the cardboard panels.

Schematics defining the braiding angle and illustrating the braiding and axial fibers are included in fig. 4. Using eq. (2), the H/A ratio for the rods manufactured in this study is 0.26. This value is slightly higher than the optimal value that has been previously reported by Hamada et al. for significantly larger rods [6].

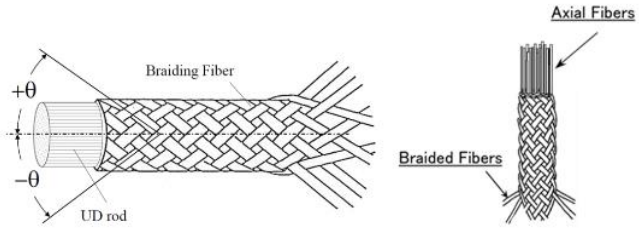

Figure 4: Schematics illustrating the braiding angle, braiding fibers, and axial fibers.

2.2 Braided Rods Manufacturing Process

The braided preform for the rods was manufactured in an industrial tubular braiding machine. The braiding process is sketched in fig. 5. The axial fiber bobbins were placed behind the braiding machine. A small stopper with a hole large enough to allow 16 fiber bundles to be guided was attached behind the braiding machine. The axial fibers were then altogether covered by the 8 braiding fiber bundles. To achieve a braiding angle of 45° for a diameter of just over 3 mm, the forward take-up speed was set to the slowest speed of 0.1 m/min (actual measured value = 0.171 m/min) and the rotation speed of the braider was set to 19.00 rpm (actual measured value = 18.12 rpm).

A close-up image of the axial fibers being covered by the braided fibers is shown on the right in fig. 5. Once the braided preform was long enough (a few meters long), it was carefully cut and wound on a bobbin in preparation for the next step of the manufacturing process.

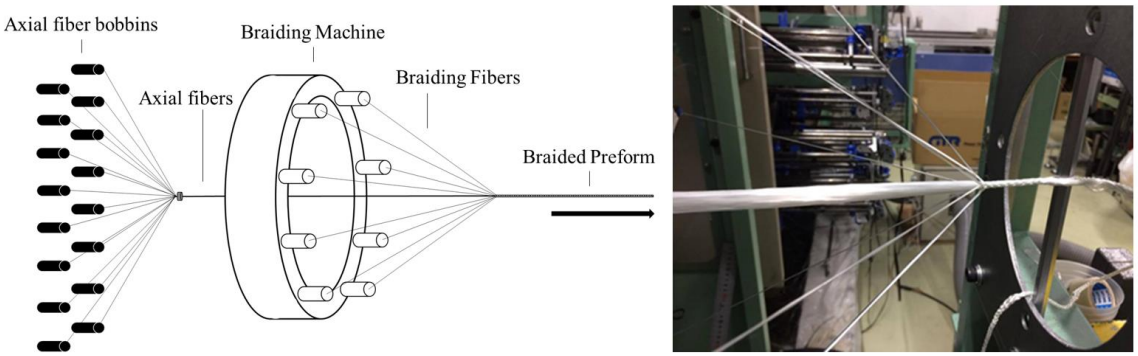

Figure 5: Sketch of the braiding process for manufacturing braided rod preforms (left), and close-up image of the braiding method where glass fiber bundles are braided around the axial fibers (right).

2.3 Resin Impregnation and Oven Curing

An epoxy resin bath was made for impregnating the dry braided preform. The epoxy resin bath was first heated to 80°C in an oven to decrease the resin viscosity for better impregnation into the fibers. The braided rod was submerged in the epoxy resin bath and inserted in a vacuum chamber oven for 10 minutes. Following the impregnation step, the wet fiber preform was hung vertically from inside the ceiling of the curing oven. A large weight was placed at the bottom to ensure that the braided structure was held straight and taught throughout the cure cycle. The rod was cured at 175°C for 4 hours. A sketch of the resin impregnation and curing configuration is included in fig. 6.

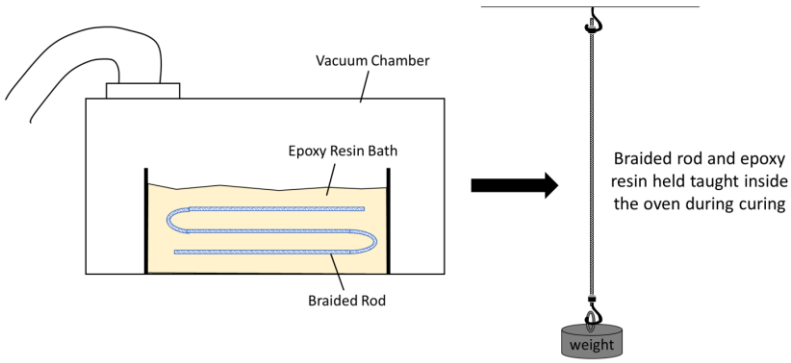

Figure 6: Sketch of the resin bath for impregnating the braided rod structure, followed by curing of the glass fiber and epoxy rod in the oven held taught with a weight.

2.4 Preparation of the crash impact panels

The cured glass fiber/epoxy rod was cut to 11.1 mm lengths and then one end of each small rod was ground to a fine tip with a 45° taper angle. A height gauge and trigonometry were used to mark the end portion of the rod that had to be ground and tapered to a tip and produce an angle of 45°. The rods were now ready to be inserted in the cardboard.

Panels with 0, 1, and 4 rods were prepared. The panels with no rods were marked as 0B-1, 0B-2, and 0B-3. The "0" signifies that no rods are inserted, and the final digit indicates the sample number. The panels with 1 rod are preceded by "1" and the panels with 4 rods are preceded by "4". A total of 3 repeats were tested for each configuration. For the samples with 1 rod, the rod was placed vertically and directly in the center. Prior to inserting the rod, a 3.4 mm diameter hole was drilled in the cardboard until just reaching the inside of the cardboard face on the other side. The tip of the tapered rod was in contact with the inside of the face. It is for this reason that the rods were cut to a length of 11.1 mm (the total thickness of the panels is 12 mm). The difference of 0.9 mm is to allow for this clearance of the cardboard face. The advantages of having a rod lying just below the inside surface of the cardboard versus being flush with the outside surface (via a thru-hole) is not known at this point. White carpenter's glue was applied both inside the hole and on the entire surface of the rod, and then the rod was carefully pushed inside until the bottom surface was flush with the bottom surface of the panel. An image of all three sample types is included in fig. 7. For the samples with 4 rods: one rod was placed directly in the center, and the other 3 were placed 15 mm from the centre, 60° apart.

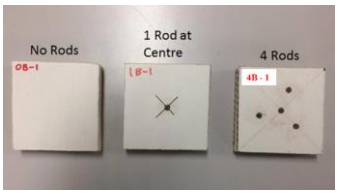

Figure 7: Crash panel samples for compression testing with 0, 1, and 4 inserted braided rods.

2.5 Compression Testing

The panels were tested in compression in a Universal Testing Machine (Instron) with a 10-ton load cell at a cross-head speed of 1 mm/min. The samples were placed directly in the center of the compression fixture. Compression testing was performed until the samples were completely crushed, at which point a steep increase in the load marked the end of the test.

3 RESULTS AND DISCUSSION

3.1 Compression Testing Results

During compression testing of the cardboard samples with no inserted rods, individual collapse of each layer was observed at different stages. The collapse of each layer is presented in fig. 8. In image A, during the earlier portion of the test, the first of two layers (top layer) is collapsing. Following the complete collapse of this layer, the load is then transferred to the second layer that subsequently collapses further in the test. The complete collapse of the first layer and the initial collapse of the second layer is shown in image B.

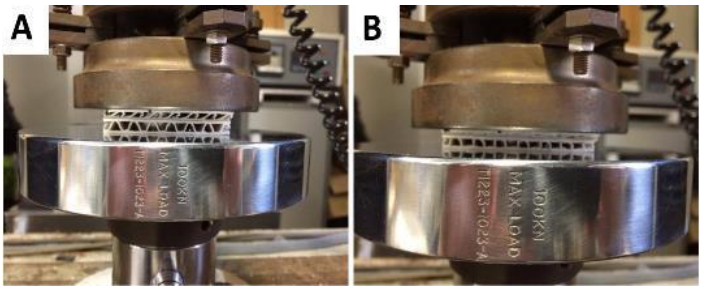

Figure 8: Collapse of the first layer (image A) and second layer (image B) during compression of the cardboard samples with no inserted rods.

The collapse of the first and second layers corresponding to images A and B, respectively, is clearly observed on the resulting load-displacement curves for 0B-1 and 0B-2 in fig. 9. At the point marked as “A”, the maximum load has been reached until the first layer collapses. At the point marked as “B”, the maximum load has been reached in the second layer before it collapses and the material is fully compressed. A third repeat was unavailable at the time of the test and is not included in the data.

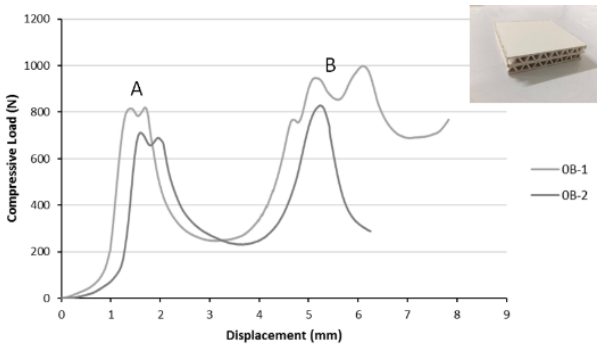

Figure 9: Load-displacement data of panels with no rods (thru-thickness direction).

The load-displacement data for the panels reinforced with 1 rod at the centre is overlapped with the previous cardboard data and presented in fig. 10-A. The maximum load sustained by these samples is significantly greater, especially in the 1B-2 and 1B-3 samples. Sample 1B-2 also best displays progressive crushing, where the load remains relatively constant until the material is fully compressed. Samples 1B-1 and 1B-3 show a decrease in the load after the maximum load value is reached (the load does not remain constant as we would expect in a tapered glass fiber rod). Further investigation of the rods and the cardboard is required to determine the root cause. Although a noticeable increase in the maximum load sustained is observed, a constant load in samples 1B-1 and 1B-3 would be optimal.

The load-displacement data for the panels reinforced with 4 rods is presented in fig. 10-B. The maximum load sustained by these samples is significantly greater than the samples with 1 rod. The maximum load reached by these samples ranges from 7000 to over 8000 N, which is approximately 4 times greater than in the samples with 1 rod as we would expect. However, once again, some samples show progressive crushing better than others. In sample 4B-2, there is progressive crushing taking place, as throughout most of crushing, the load remains relatively constant at about 8000 N. In sample 4B-3, the load decreases from approximately 7000 N to 5500 N, and the progressive crushing is not quite as good as in sample 4B-2. In sample 4B-1, the load decreases from 7200 N to 4000 N, and displays the least amount of progressive crushing. Despite the maximum load that is reached by the 4-rod samples, a more constant load throughout crushing is desirable.

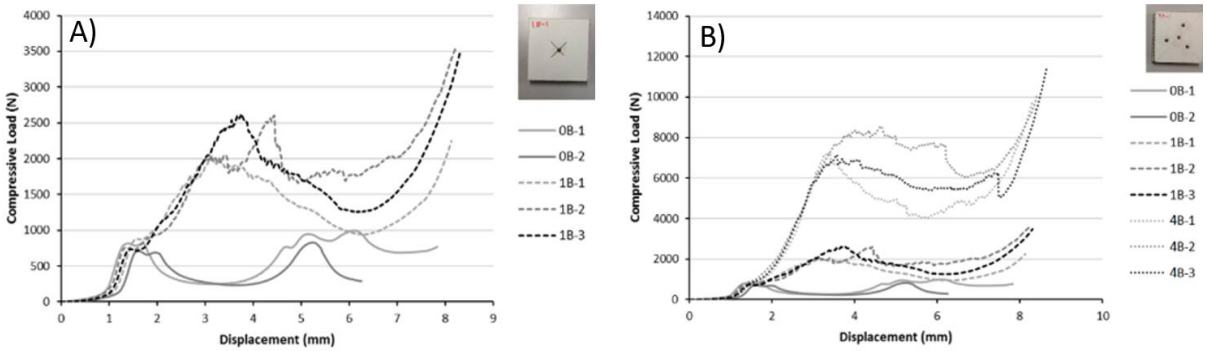

Figure 10: A) Load-displacement data including panels with 1 rod (thru-thickness direction); B) Load-displacement data including panels with 4 rods (thru-thickness direction).

3.2 Fiber Splaying Observations

After compression testing, the surfaces of the panels were observed for any signs of progressive crushing. Figure 11 includes images of the top (left column) and bottom (right column) surfaces of the crushed panels containing 1 braided rod. The top surface of the panel corresponds with the tapered end of the rod. From the images, it is evident that the rods have crushed as some of the fibers have penetrated through the top surface of the cardboard. However, despite it being difficult to tell with the cardboard surrounding the rods, it appears that the crushed rods do not show any significant signs of fiber splaying on the top surface. The locations of the glass fiber residue from the rods are concentrated within a small perimeter. When comparing the size of the small white circles on the top and bottom surfaces, there is not much difference in their size. This size comparison becomes apparent when observing the failure surfaces of the panels with 4 rods.

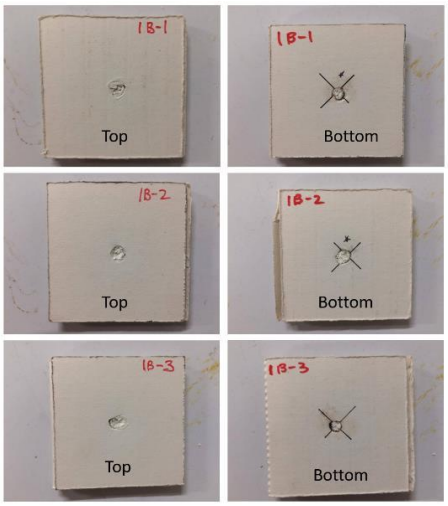

Figure 11: Top and bottom surfaces of panels with one rod after compression. The top surface refers to the tapered end of the glass rod.

When observing the bottom surfaces, some signs of damage are also present, especially in sample 1B-2. The presence of damage on the bottom surface of the rods is likely due to the propagation of cracks along the axis of the rods. This observation, and that there is very little fiber splaying on the top surface, can explain why the load decreased after reaching a maximum and that progressive crushing did not occur.

Images of the top and bottom surfaces of the crushed panels with 4 rods are presented in fig. 12. Additional markings have been included on the images for identification of important features. Rods where a significant amount of fiber splaying is present are marked with a circle. The rods that show a moderate level of fiber splaying are marked by a square. Each rod as viewed from the top and bottom surface has been numbered accordingly. The rods that do not show signs of fiber splaying and progressive crushing have not been marked or numbered. In sample 4B-1, only one rod has fiber splaying present as seen on the top surface. It is also interesting to see that the bottom side of the rod is also practically undamaged compared to its initial state before the compression test. All the other rods that did not splay also show signs of damage on the bottom surface. Clearly, the rod that has splayed has been successful in crushing progressively, and most of the energy absorbed during crushing as the fibers splayed outwards. No other sources of damage that would limit the energy absorption of the rods is present in the form of axial cracks (as seen from the bottom surface). As only one rod was optimally crushed out of the four, this is likely the reason that the load-displacement curve of the 4B-1 sample shows a decreasing load after reaching the maximum value.

Similar observations are made in samples 4B-2 and 4B-3. However, in sample 4B-2, one rod has shown excellent fiber splaying and the other three have shown a moderate amount. This supports the desirable crushing behavior of this sample as seen from the load-displacement curves in fig. 10-B. The more rods display fiber splaying, the better the crushing load is maintained in the samples. Samples 4B-1 and 4B-3 show similar features on the panel surfaces, and it is not clear why sample 4B-3 sustains the load better than sample 4B-2.

It is uncertain whether the H/A ratio for the rods in this study is too high and should be reduced to the optimal value of 0.12 to 0.13 that has been previously reported for 12 mm diameter rods. Exploring alternate H/A ratios is certainly of interest for future studies.

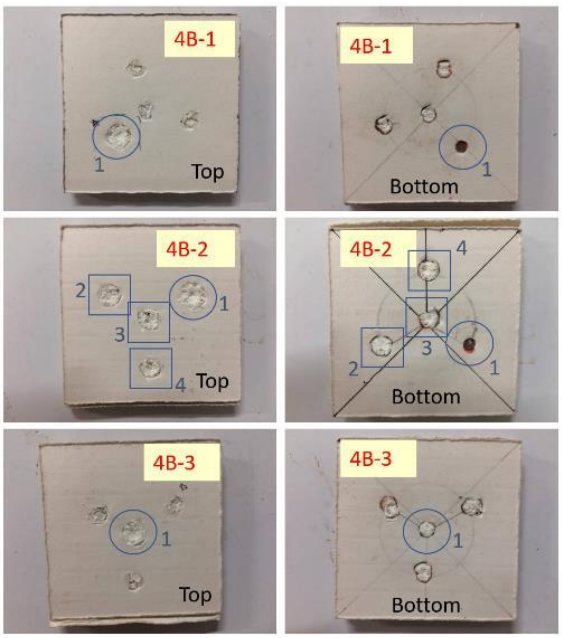

Figure 12: Top and bottom surfaces of panels with four rods after compression. the top surface refers to the tapered end of the glass rods.

3.3 Optical Microscopy Observations of Crushed Rods

Optical microscopy images of two different rods from crushed panels reinforced by 1 rod (1B type sample) are shown in fig. 13.

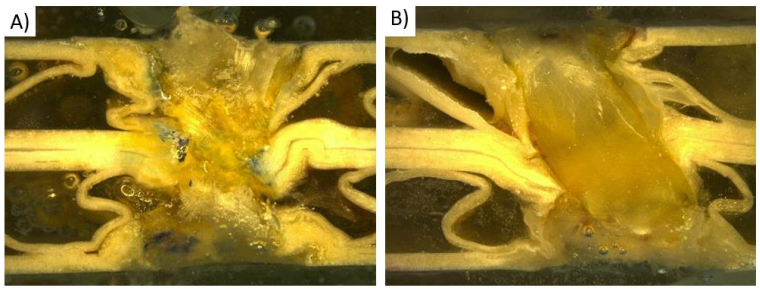

Figure 13: Cross-section images of two different rods from samples reinforced with one rod (1B sample).

In the first image (A) of fig. 13, the tapered end of the rod is located at the bottom. On both ends of the rod, it appears that some damage is present. The rod appears vertical throughout the thickness of the cardboard, however significant internal damage is likely present in the rod as one end of the rod cannot be clearly distinguished from the other. In the prior observations of the 1 rod-reinforced panels, no rods clearly showed significant fiber splaying, and all rods showed signs of damage on the bottom surface. These signs are all visible in the first image. In the second image (B) of fig. 13, the tapered end of the rod is also located at the bottom. This rod is clearly on an angle, and has been displaced from its vertical orientation during compression testing. Deformation of the surrounding cardboard probably tilted the rod. When the load is applied to a rod on an angle, proper progressive crushing cannot occur. The rod must remain vertical throughout crushing for maximum energy absorption. It is uncertain if the rod in the first image is also tilted as viewed from other directions.

An image of a rod that displayed a lot of splaying from a 4-rod sample is shown in fig. 14. The tapered end of the rod is located at the bottom of the image. It can be clearly seen that the tapered end of the rod shows a lot of fiber splaying – many fibers spread outwards. The bottom end of the rod (top of the image) also appears undamaged with a clear cylindrical shape. For some unknown reason, the bottom end of the rod is also slightly below the surface of the cardboard. Rods that exhibit progressive crushing should only splay from one end and remain undamaged on the other end – supporting the previous observations.

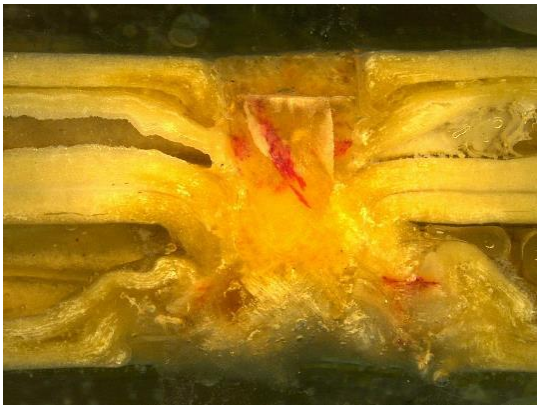

Figure 14: Cross-section image of a rod from a sample reinforced with four rods (4b sample).

4 CONCLUSIONS

The objective of this study was to manufacture crash impact attenuation panels made from cardboard and braided unidirectional glass fiber rods. Their crushing behavior was investigated by

performing compression tests. The braided rod preforms consisting of axial and braided fibers were first fabricated with a tubular braiding machine and then impregnated with epoxy resin and cured. The rods were inserted in the cardboard, and the crushing behaviour of panels reinforced with 0, 1, and 4 rods was assessed. The main findings from this study are as follows:

- The load-displacement curves of cardboard panels with no rods reaches two peaks, corresponding to the collapse of each individual cardboard layer.
- The maximum load sustained increases with the number of reinforcing rods. Panels with 1 rod are significantly stronger than those with no rods, and panels with 4 rods reach a maximum load that is approximately 4 times greater than in panels with 1 rod.
- Despite being stronger, panels with 1 rod and certain panels with 4 rods show a considerable decrease in load during crushing. Some samples show signs of progressive crushing more than others, where the load remains constant.
- Surface observations reveal that the panels that best sustain higher loads during crushing are those that contain multiple rods characterized by fiber splaying. Fiber splaying was identified by the size of the glass fiber circular patterns that remained of the crushed rods as seen from the top surface of the panels.
- Optical microscopy images show that damage may be present in the rods that do not splay well at one end. In addition, the rods that are tilted from the vertical due to deformation of the surrounding cardboard also do not splay well.

ACKNOWLEDGMENTS

The authors would like to acknowledge the support of Mr. Tadashi Uozumi from Gifu University for his support in the operation of the braiding machine. The authors would also like to acknowledge Daiwa Itagami Co., Ltd. for supplying the cardboard panels, and Nitto Boseki Co., Ltd. for supplying the glass fiber.

REFERENCES

[1] Production Statistics, Organisation Internationale des Constructeurs d'Automobiles (OICA). (2017). *2015 Production Statistics.* Retrieved 27 April, 2017, from http://www.oica.net/category/production-statistics/2015-statistics/

[2] Greenhouse Gas Emissions, United States Environmental Protection Agency. (2017). *Transportation Sector Emissions.* Retrieved 27 April, 2017, from https://www.epa.gov/ghgemissions/sources-greenhouse-gas-emissions#transportation

[3] MIT News, Massachussetts Institute of Technology. (2013). *Study: Air pollution causes 200,000 early deaths each year in the U.S.* Retrieved 28 April, 2017, from http://news.mit.edu/2013/study-air-pollution-causes-200000-early-deaths-each-year-in-the-us-0829

[4] U.S., Newsweek. (2015). *U.S. Traffic Deaths, Injuries and Related Costs Up In 2015.* Retrieved 28 April, 2017, from
http://www.newsweek.com/us-traffic-deaths-injuries-and-related-costs-2015-363602

[5] Hamada, H., Coppola, J.C., Hull, D., Maekawa, Z., & Sato, H. (1992). Comparison of energy absorption of carbon/epoxy and carbon/PEEK composite tubes. *Composites*, 23, 4, 245-252.

[6] Hamada, H., Kameo, K., Sakaguchi, M., Saito, H., & Iwamoto, M. (2000). Energy-absorption properties of braided composite rods. *Composites Science and Technology*, 60, 723-729.

[7] Hull, D. (1991). A Unified Approach to Progressive Crushing of Fibre-Reinforced Composite Tubes. *Composites Science and Technology, 40, 377-421.*

[8] Yasuda, S. (2017). Fracture Behavior of Textile Composites (MASc). Kyoto Institute of Technology.